Sensors and Actuators B 141 (2009) 205–209

Contents lists available at ScienceDirect

Sensors and Actuators B: Chemical

journal homepage: www.elsevier.com/locate/snb

Hydrogen peroxide electrochemical detection for the development of protein film-modified sensor

Yuanbiao Qiao[a], Guang Yang[a], Fangfang Jian[b], Yongqi Qin[b], Lirong Yang[a,*]

[a] College of Materials Science and Chemical Engineering, Zhejiang University, Zhejiang 310027, PR China
[b] New Materials and Function Coordination Chemistry Laboratory, Qingdao University of Science and Technology, Shandong 266042, PR China

ARTICLE INFO

Article history:
Received 16 March 2009
Received in revised form 2 May 2009
Accepted 15 May 2009
Available online 27 May 2009

Keywords:
Protein film voltammetry
Zr^{4+}-nucleotide nanocomposite
Hydrogen peroxide sensor

ABSTRACT

A protein thin film-modified electrode sensor, that features both generalizability and simplicity in design toward reagentless detection of hydrogen peroxide with high sensitivity and reliability, is reported here. Within this electrode device, the film active material of the nanocomposite of myoglobin and zirconium (iv) ion-adenosine monophosphate dianion particles forming *via* monolayer adsorption of protein, is fabricated on a glassy carbon surface using self-assembly technique. The electrode modification helps in facilitating the direct electron transfer kinetics of protein at the formal potential ($E^{\circ\prime}$) of 12.3 mV *versus* SHE (pH 7.0). As a result, the potential applied in H_2O_2 determination through reduction can be shifted to −3.7 mV, a useful characteristic for further applications. Furthermore, the electrode configuration provides sufficient operational stability for sensing. Detection limit of 0.06 μM and the linear calibration range up to 148.47 μM H_2O_2 are obtained for this sensor. The sensor assay can retain a value of 91.7% initial activity within 1 month.

1. Introduction

The development of high sensitive and selective methods for H_2O_2 determination is a very important analytical task in many fields, with particular emphasis on biosensors based on oxidase enzymes [1]. Oxidase enzymes can catalyze H_2O_2 reduction and allow the direct electron transfer between active site and electrode surface [2,3]. In the last years, the number of sensors measuring H_2O_2 increased considerably. A variety of materials, including nanoparticles [4], sol–gels [5], polymers [6] and carbon nanotubes [7], have been employed to immobilize enzymes. The use of the materials for immobilization admits a low-potential measurement of H_2O_2 with advantageous analytical characteristics, such as little interfacial problem, high limiting sensitivity, and large dynamic range [4–7]. These sensors, even if sensitive, suffer from shortcomings for low stability and limited binding of enzymes to solid surface [8]. Moreover, the introduction of enzymes into films may increase configurational complexity of sensors. Till now, there are several challenges concerning the simplification of fabrication and the retention of activity for sensors to be made more robust. The development of reliable materials is crucial, and that of new fabrication strategies is still a prevailing subject.

Electroconductive zirconia (ZrO_2) and zirconium phosphate (α-ZrP) have already been employed as good matrices for immobilization of proteins [9,10]. But their little mechanical rigidity together with the low affinity toward proteins binding has restricted further applications [8,11,12]. Generally, the structure of proteins in immobilization is a genuine concern not only because of apprehensibility of binding mechanisms but also for the potentiality of better practical uses. Recent work [10] has demonstrated that the protein structure may undergo a slight unfolding with adsorption onto ZrO_2 nanoparticles. To tackle these problems, materials grafting with DNA [11] and nucleotide [13] appear promising candidates for the development of sensors. The genetic groups, that link through chemical bonding [14] in materials, can be considered as the systems for connecting proteins to electrode and for binding proteins with good compatibility. So far, DNA has been exploited electron transfer enhancement of proteins [15,16]. Despite of this, entrapment of proteins with the matrices of mere nucleic acids leads to the obtained films with drawbacks, such as low stability [17] and little diffusibility [18], due to flexible and polymorphic structural features of nucleic acids. Our previous study [13] has reported that nanogranules of Zr^{4+}-uridine monophosphate dianion monohydrate, $Zr(UMP)_2{\cdot}H_2O$, can be easily synthesized under mild conditions. The film of myoglobin (Mb) supported by $Zr(UMP)_2{\cdot}H_2O$ reveals excellent analytical performances in H_2O_2 detection, as characterized by electrochemical method. Moreover, Mb folds into a native-like structure after immobilization.

Here the preparation of new nanoparticles of Zr^{4+}-adenosine monophosphate dianion, abbreviated as $Zr(AMP)_2$, is introduced in order to obtain its stable composite with Mb, to construct the electrode building based upon nanocomposite film modification, and

* Corresponding author. Tel.: +86 0571 87952009; fax: +86 0571 87952363.
E-mail address: lryang@zju.edu.cn (L. Yang).

0925-4005/$ – see front matter © 2009 Elsevier B.V. All rights reserved.
doi:10.1016/j.snb.2009.05.015

to achieve H_2O_2 sensing with improved properties. Due to high affinity between Mb and $Zr(AMP)_2$, the nanocomposite refereed to $Zr(AMP)_2$–Mb, can be easily formed *via* monolayer adsorption of Mb molecules onto particles, indicating a reliable film-material preparation. Using self-assembly, it is able to fabricate the electrode surface with simplicity. The obtained electrode configuration has been characterized and used for H_2O_2 detection. The most advantage within electrode building is that noncovalently bound nanocomposite, which is stable against washing-off in water, may be easily purified.

2. Experimental

2.1. Preparation of $Zr(AMP)_2$ nanoparticles

Colorless nanoparticles of $Zr(AMP)_2$ are obtained by the reaction of zirconium tetrachloride ($ZrCl_4$, Merck-Schuchardt) with adenosine monophosphate disodium ($AMPNa_2$, Serve) in a stoichiometric ratio of 1:2 (mol/mol). The reaction is carried out in dilute solution of cetyl trimethylammonium bromide (0.1% (w/w) CTAB, Beijing Chemical Plant) [13]. After fleet stirring (8000 rpm) for 10 h at 4 °C, the suspension is centrifuged at 13,300 rpm for 15 min. The pellets are washed with ethanol, dried and then characterized.

2.2. Adsorption of Mb on $Zr(AMP)_2$ particles

In order to examine Mb (IEP 7.1) [19] adsorption on particles as a function of protein concentration, a volume of 80 μl of Mb aqueous solution (C = 14 mg/ml) is added to colloidal suspension of particles (C = 0.5 mg/ml, V = 1.0–6.0 ml, pH 7.0). The mixtures are incubated for 5 h at room temperature, and then adsorbed protein is recovered by centrifuging at 13,300 rpm for 15 min. The pellets are washed, and the supernatants are collected for determination of free protein. Protein concentration is assayed by UV spectra (λ = 409 nm, ε = 160,000 M^{-1} cm^{-1}). The amount of adsorbed protein is calculated from the difference between the value of protein concentration in initial solution and that in supernatants.

2.3. Characterizations and electrochemical experiments

The X-ray photoelectron spectroscopy (XPS) is recorded on an ESCLABMK II spectrometer (VG Co., UK) using the Al Kα radiation. The particles are dispersed in pure water. A drop of suspension solution of particles (1.0 mg/ml) is placed onto a clean silicon wafer (0.5 cm × 0.5 cm) and dried. The X-ray powder diffraction (XRPD) is taken with a computerized Philips PW 1710 diffractometer in a continuous mode over the 2θ range of 3–50°. Electrochemical impedance spectroscopy (EIS) is done at a potential of −3.7 mV *versus* SHE, using an EGG-283 potentiostat/galvanostat (Princeton Applied Research). Atomic force microscopy (AFM) is carried out on a Nanoscope III_a multimode digital microscope (Santa Barbara, CA, USA) in a taping mode. The vibrating frequency range of 0–273.77 kHz and the scan rate of 1 Hz are employed. A volume of 100 μl of suspension solutions (0.1 mg/ml) of $Zr(AMP)_2$ and $Zr(AMP)_2$–Mb is dropped on the mica (⌀ 5 mm) surfaces, and the films are formed by drying overnight. All images are recorded at 20 ± 2 °C, and relative humidity ≤ 55%.

Cyclic voltammetry (CV) is performed on an Autolab PGSTAT-30 digital potentiostat/galvanostat (Eco Chemie BV, Utrecht, Netherlands), using anaerobic potassium phosphate (10 mM, pH 7.0) as base electrolyte. A three-electrode system, which is consisting of a glassy carbon edged plane (⌀ 2 mm), a platinum sheet (0.8 cm × 0.8 cm) and an Ag/AgCl tip (1.0 M KCl), respectively, is employed. All potentials except specific statement are quoted *versus* the Ag/AgCl electrode (236.3 mV, at 20 °C). The procedure for the film electrode preparation is followed by immersing a clean glassy carbon electrode into colloidal suspension of $Zr(AMP)_2$–Mb (0.1 mg/ml) for 20 min, drying under argon atmosphere for 1 h, and rinsing the electrode surface for three times with potassium phosphate. The $Zr(AMP)_2$ film electrode is obtained with similar method.

3. Results and discussion

3.1. Characterizations of prepared $Zr(AMP)_2$ particles

The Zr and P mass percent is examined by XPS (Fig. 1). It gives a molar ratio of 1:2 between Zr and P, which indicates evidently that this compound has a molecular formula of $Zr(AMP)_2$ (*Anal.* (%): P 7.75 and Zr 11.41; *Found* (%): P 7.78 and Zr 11.38). The XRPD pattern shows wide and unseparated peaks, revealing little crystallinity for material (*inset*). The surface characteristic for a deposit of material is tested by AFM (Fig. 2a). As can be clearly seen, the plate-like nanoparticles with a diameter and a height of about 60 and 20 nm, respectively, are observed in the 2 μm/2 μm image. The deposit displays floccular and collapsing morphology, probably because of low fracture toughness [12], and little crystallinity as characterized with XRPD.

3.2. Adsorption isotherm

The Mb adsorption test is done with colloidal suspension of $Zr(AMP)_2$ particles. The inorganic particles with nucleotide group locating at the surfaces are negatively charged at the pH used in experiment. It is suggested that the presence of various lysine residues distributed over Mb surface may be responsible for electrostatic interactions with negatively charged particles [10]. In this study, the dependence of Mb adsorption on its concentration is evaluated at different protein/support ratios under same conditions, and the result is shown in Fig. 3. A plateau is seen at 0.24 ± 0.01 mg Mb bound/mg support, which is comparable with those for Mb adsorbed on phosphate-grafted ZrO_2 particles (0.28 mg Mb bound/mg support) [10]. According to the Langmuir model [9], the plateau for a maximal Mb adsorption capacity is compatible with a monolayer of the molecules on particles.

It is a special likelihood for the preparation of stable nanocomposite with ease due to high affinity of particles toward Mb binding. The product is treated by successive centrifugation and washing, in order to allow the separation of non-adsorbed protein. After above steps for purification, a uniform protein structure is realized in

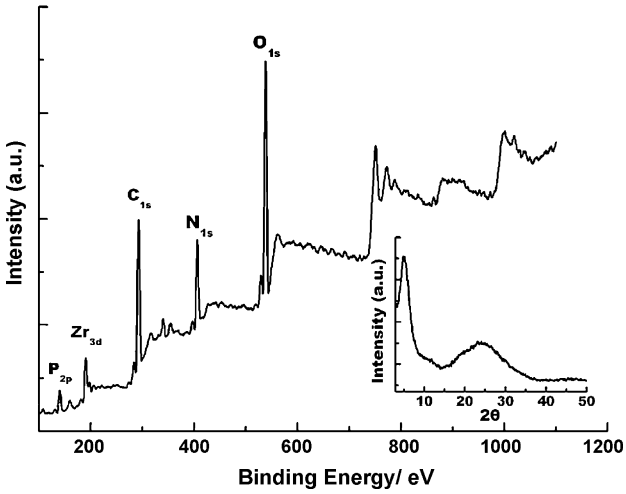

Fig. 1. X-ray photoelectron spectroscopy pattern of synthesized particles. The P and Zr mass contents are calculated from the peak area ratios using cofactors of P_{2p} 0.39 and Zr_{3d} 2.10, respectively. Inset: X-ray powder diffraction pattern of particles on Ti foil.

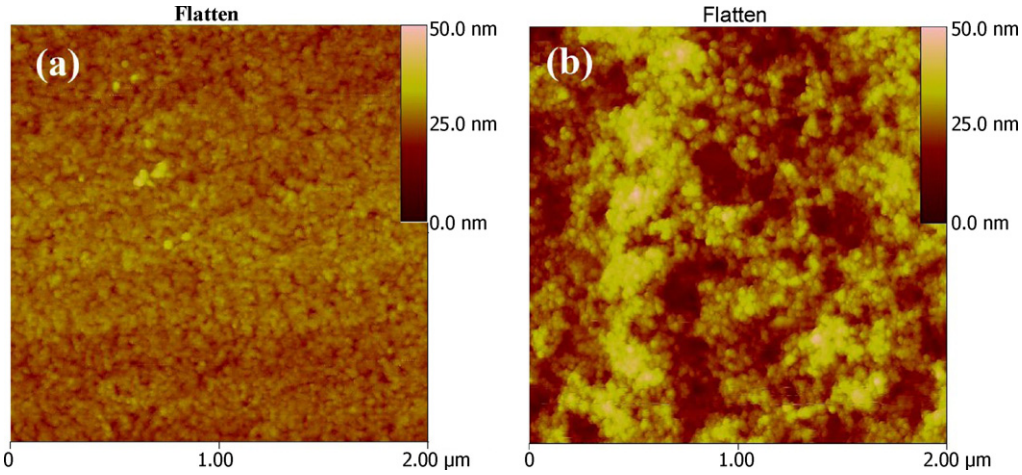

Fig. 2. The 2 μm/2 μm atomic force microscopy images for $Zr(AMP)_2$ (a) and $Zr(AMP)_2$–Mb (b).

an absolute immobilization state. The use of nanocomposite with identical compositions, a reliable method for film-material preparation, is yet failed to solve at present. In this case, a quantitative study is performed with immobilized Mb, and the resulted nanocomposite at a maximal Mb adsorption capacity is used throughout all tests.

3.3. Electrochemical impedance spectroscopy (EIS) studies

EIS is used to monitor the growth of films with the redox probe of $Fe(CN)_6^{3-/4-}$ (0.1 mM) in potassium phosphate (pH 7.0). The experiments are performed at −3.7 mV *versus* SHE because this is the potential used in H_2O_2 determination. Fig. 4 shows the impedance spectra in the form of Nyquist diagrams at electrode surface. It is seen that the presence of electroconductive $Zr(AMP)_2$ and $Zr(AMP)_2$–Mb dramatically modifies the EIS response of the system. For the films of both $Zr(AMP)_2$ and $Zr(AMP)_2$–Mb, a semicircle is clearly observed at high frequencies, where the diameter is related to the films resistance (R_{ct}) [20]. By analyzing low frequency region, it is possible to observe a transition from semi-infinite diffusion (in the case of non-modified electrode) to finite diffusion for film-modified electrodes. On the other hand, comparing the diameter of the semicircle presented in EIS, it is clear that the R_{ct} for $Zr(AMP)_2$–Mb film is higher than that of $Zr(AMP)_2$ film, similar variations of which have also been observed for the films of ZrO_2 after adsorption by hemoglobin and horseradish peroxidase [4,11] or the film of α-ZrP doped with Mb [21].

The Mb adsorption is also testified by AFM measurement (Fig. 2b). It is seen in image that the presence of protein influences the surface morphology of particles greatly. A highly irregular-stacking structure, consisting of much globular aggregates compared to those of $Zr(AMP)_2$, is identified for $Zr(AMP)_2$–Mb. The maximal deposit height is about 60 nm.

3.4. Electrochemical experiments

CV is performed to assess redox of the nanocomposite assemblies on electrode surface as characterized in 10 mM potassium phosphate, pH 7.0 (Fig. 5). The CV diagram presents two obvious peaks, corresponding to the Mb reduction and oxidation. At a scan rate of 20 mV s^{-1}, the formal potential ($E^{\circ\prime}$), defined as the average of anodic potential (E_{pa}) and cathodic potential (E_{pc}), is calculated to be −0.224 V (12.3 mV *versus* SHE), and the peak separation ΔE_p, (E_{pa}–E_{pc}) is 102 mV. The reduction current (I_{pc}) and integrated charge (Q) of 24.78 nA and 0.26 μC, respectively, is obtained for $Zr(AMP)_2$–Mb film electrode at the scan rate. According to the relation [22]: $Q = nFA\Gamma^*$ (n, F, A, Γ^* represents electron transfer number,

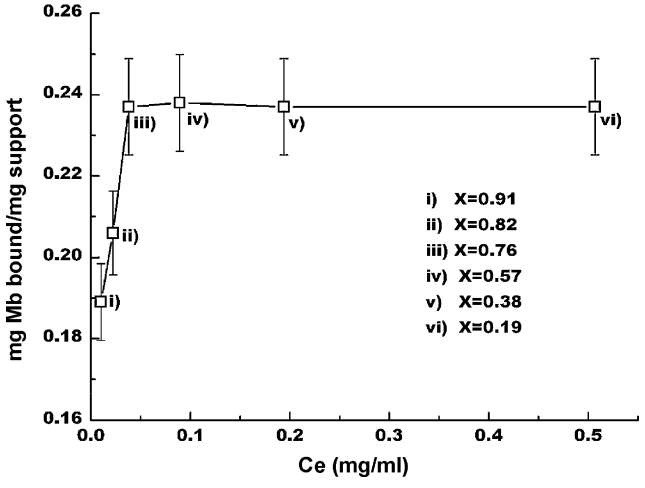

Fig. 3. Adsorption isotherm of Mb onto $Zr(AMP)_2$ particles (pH 7.0, T = 20 °C, t = 5 h, X = Mb bound/Mb total, Ce = residual concentration of Mb in solution after adsorption).

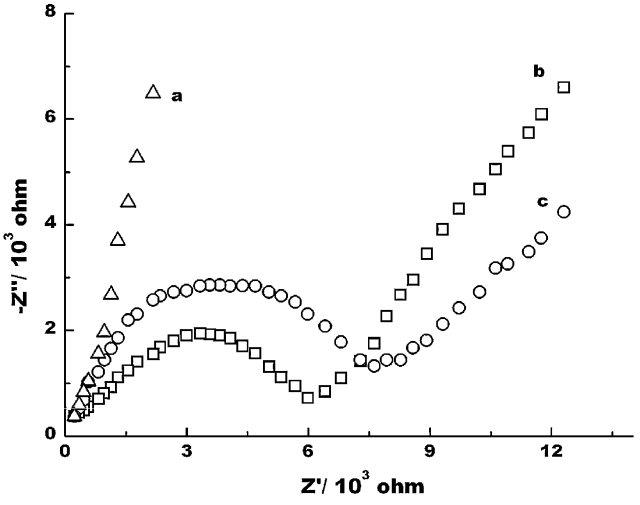

Fig. 4. Impedance spectroscopy spectra, proving the immobilization of colloidal $Zr(AMP)_2$ (b) and $Zr(AMP)_2$–Mb (c) layers on electrode surface as compared to bare electrode (a).

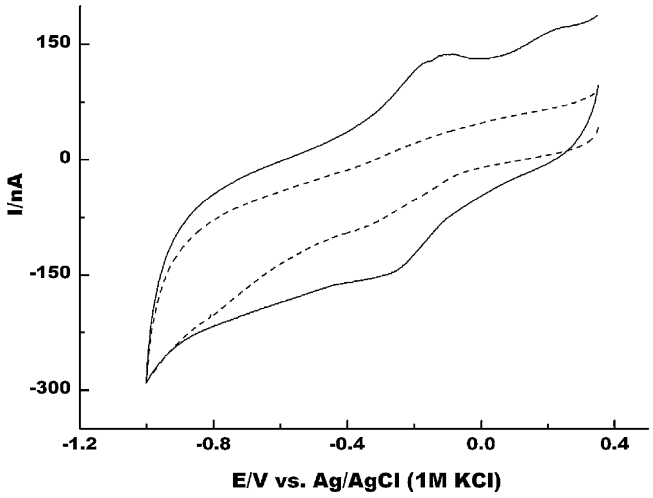

Fig. 5. Cyclic voltammograms for $Zr(AMP)_2$–Mb (*solid line*) and $Zr(AMP)_2$ (*dash line*) films on glassy carbon electrode (10 mM potassium phosphate, pH 7.0, at 0.02 V s^{-1}, and 20 °C).

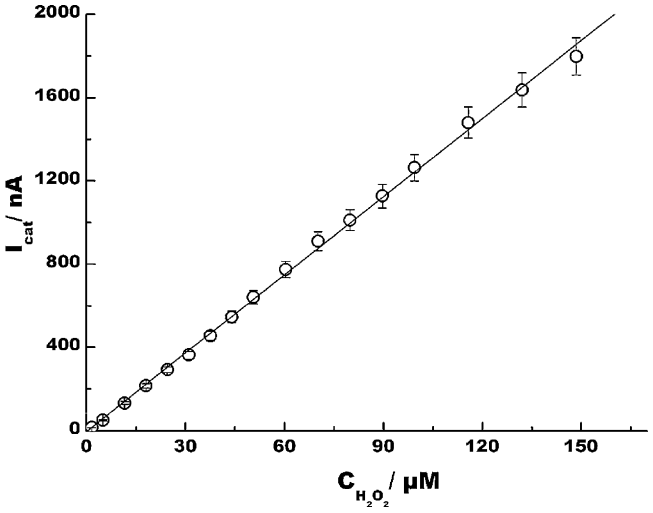

Fig. 7. Plot of I_{cat} *versus* $C_{H_2O_2}$ for H_2O_2 sensor. Line is the calibration result.

Faraday's constant, electrode area and electroactive concentration of Mb, respectively), the Γ^* is found to be 0.90×10^{-10} mol cm^{-2} for $Zr(AMP)_2$–Mb film electrode. In consideration with the Mb monolayer amount of 0.47×10^{-10} mol cm^{-2} and the crystallographic dimension of 2.5 nm × 3.5 nm × 4.5 nm [23], about two layers of nanocomposite fabricated on electrode surface keep active when Mb is bound to particles *via* monolayer adsorption.

3.5. H_2O_2 determinations

The H_2O_2 sensing for $Zr(AMP)_2$–Mb film electrode is studied by using CV technique (Fig. 6). Within a potential window from −1.0 to 0.4 V, $Zr(AMP)_2$ film electrode gives no response when dipping in H_2O_2 solution. However, $Zr(AMP)_2$–Mb film on electrode displays obvious reduction peaks at the E_{pc} of about −0.24 V (−3.7 mV *versus* SHE). The height for reduction peaks is enhanced greatly, while that for corresponding oxidation peaks is decreased and ultimately disappeared when H_2O_2 concentration ($C_{H_2O_2}$) is increased. The difference in the reduction potentials with/without H_2O_2 is about 30 mV. These results are in accordance with a fast electrocatalysis for H_2O_2 reduction [24]. Defined as the difference between the I_{pc} in the presence and that in the absence of H_2O_2, the electrocatalytic current (I_{cat}) varies linearly with $C_{H_2O_2}$ in the beginning and levels off thereafter, revealing a catalytic kinetics in Michaelis–Menten manner. The $C_{H_2O_2}$ at the lever-off response is 164.9 μM for $Zr(AMP)_2$–Mb film. A Lineweaver–Burke plot for I_{cat} *versus* $C_{H_2O_2}$ gives an apparent Michaelis–Menten constant (K_M) of only 92.46 μM for this film.

Fig. 7 shows the calibration curve obtained at −0.24 V fixed potential for the sensor developed in this work. CV is sampled after a 30-s delay when H_2O_2 is added in potassium phosphate (pH 7.0). The response signal for sensing refers to the I_{cat} obtained with $Zr(AMP)_2$–Mb thin film-modified electrode in H_2O_2 solution. The obtained detection limit is 0.06 μM (calculated as three times the Standard Deviation of phosphate blank), and the linear calibration range is extending up to 148.47 μM. The regression equation is: I_{cat} (nA) = −2.08 + (12.51 ± 0.12) × $C_{H_2O_2}$ (μM), r = 0.999. There were already reported Mb films for H_2O_2 sensing [13,25], having the detection limit of 1.52 and 4.00 μM, and the linear range of 180.14 and 1500 μM, respectively. The sensor in this work gives very low limit of detection, indicating high sensitivity. The dynamic parameter for $C_{H_2O_2,d.r.}/C_{H_2O_2,d.l.}$ (d.r. = dynamic range, and d.l. = detection limit) is extending over 1.4 and 0.8 orders of magnitude as compared to those for reported sensors, and this may be probably explained by the fact that the conductivity of reported films is dif-

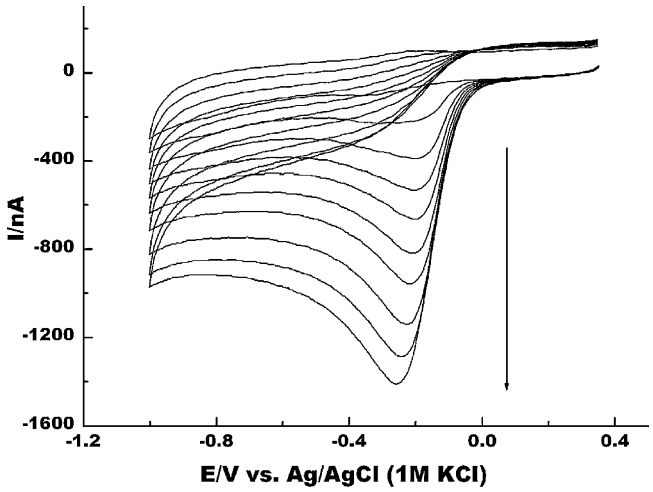

Fig. 6. Cyclic voltammograms for $Zr(AMP)_2$–Mb film electrode in 0.00, 37.20, 60.70, 84.19, 107.69, 139.02, 178.18, 256.50, 299.57 and 393.56 μM H_2O_2 solutions, respectively (*from up to down*) at 0.02 V s^{-1}, and 20 °C.

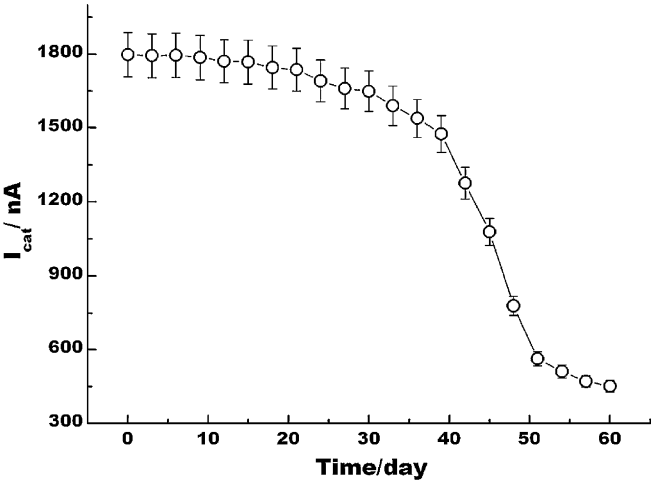

Fig. 8. Detection stability for sensor (148.47 μM H_2O_2 in potassium phosphate, at 0.02 V s^{-1}, and 20 °C).

fered from that of self-assembly film in this work. It is known that an electrode modification in the self-assembly process can make less overpotential of reduction, and can result in facilitated kinetics and enhanced activity of immobilized protein. Also, high immobilization efficiency of protein *via* monolayer adsorption, may contribute to improving analytical performances of our sensor fabrication.

The electrode Relative Standard Deviation (R.S.D.) for five parallel determinations is 3.2%, which is comparable with those obtained from other Mb films [4,11,13,25]. The sensor has a good stability when working inside dynamic range (Fig. 8). A decrease in activity is only 8.3% after the H_2O_2 (148.47 μM) assays for 10 times at an interval of 3 days. No significant change is seen in storage conditions (potassium phosphate 7.0, 4 °C, dark). This sensor can retain only 25% original activity beyond 2 months because of the severe desorption of protein.

4. Conclusion

In this work, the fabrication and electrochemical characterization of electrode sensor, based upon $Zr(AMP)_2$–Mb nanocomposite film modification, were reported. The film active material has achieved very stable adsorption and connection to electrode, as proved by impedance spectroscopy, atomic force microscopy and cyclic voltammetry, respectively. The sensor gives improving detection limit (down to 0.06 μM) and dynamic range (up to 148.47 μM) for H_2O_2 measurement. The parallel H_2O_2 sensing is reliable because the nanocomposite, which is apart from the mixture with non-immobilized protein, can be obtained in a way of repeatability. It is propose that this kind of film-material preparation, together with simple fabrication technique may be commercially developed toward the construction of stable and sensitive sensor platforms.

Acknowledgements

The authors thank for the financial supports on the Chinese National Natural Science Foundation (Grant No. 20606030 and 20336010), Key Project of Chinese National Programs for Fundamental Research and Development (Grant No. 2003CB716008), and Hi.-Tech. Research and Development Program of China (Grant No. 2006AA02Z238).

References

[1] T. Ruzgas, E. Csöregi, J. Emnéus, L. Gorton, G. Marko-Varga, Peroxidase-modified electrodes: fundamentals and application, Anal. Chim. Acta 330 (1996) 123–138.
[2] A. Lindgren, T. Ruzgas, L. Gorton, E. Csöregi, G.B. Ardila, I.Y. Sakharov, I.G. Gazaryan, Biosensors based on novel peroxidases with improved properties in direct and mediated electron transfer, Biosens. Bioelectron. 15 (2000) 491–497.
[3] S.S. Razola, B.L. Ruiz, N.M. Diez, H.B. Mark Jr., J.M. Kauffmann, Hydrogen peroxidase sensitive amperometric biosensor based on horseradish peroxidase entrapped in a polypyrrole electrode, Biosens. Bioelectron. 17 (2002) 921–928.
[4] S.Q. Liu, Z.H. Dai, H.Y. Chen, H.X. Ju, Immobilization of hemoglobin on zirconium dioxide nanoparticles for preparation of a novel hydrogen peroxide biosensor, Biosens. Bioelectron. 19 (2004) 963–969.
[5] X.H. Chen, Y.B. Hu, G.S. Wilson, Glucose microbiosensor based on alumina sol–gel matrix electropolymerized composite membrane, Biosens. Bioelectron. 17 (2002) 1005–1013.
[6] O. Ngamma, A. Morrin, S.E. Moulton, A.J. Killard, An HRP biosensor using sulphonated polyaniline, Synth. Met. 153 (2005) 185–188.
[7] V.S. Tripathi, V.B. Kandimalla, H.X. Ju, Amperometric biosensor for hydrogen peroxide based on ferrocenebovine serum albumin and multiwall carbon nanotube modified ormosil composite, Biosens. Bioelectron. 21 (2006) 1529–1535.
[8] A.A. Karyakin, E.E. Karyakina, Prussian blue-based artificial peroxidase as a transducer for hydrogen peroxide detection, application to biosensors, Sens. Actuators B: Chem. 57 (1999) 268–273.
[9] F. Bellezza, A. Cipiciani, M.A. Quotadamo, Immobilization of myoglobin on phosphate and phosphonate grafted-zirconia nanoparticles, Langmuir 21 (2005) 11099–11104.
[10] F. Bellezza, A. Cipiciani, M.A. Quotadamo, S. Cinelli, G. Onori, S. Tacchi, Structure, stability, and activity of myoglobin adsorbed onto phosphate-grafted zirconia nanoparticles, Langmuir 23 (2007) 13007–13012.
[11] Z.Q. Tong, R. Yuan, Y.Q. Chai, S.H. Chen, Y. Xie, Direct electrochemistry of horseradish peroxidase immobilized on DNA/electrodeposited zirconium dioxide modified gold disk electrode, Biotechnol. Lett. 29 (2007) 791–795.
[12] R. Benzaid, J. Chevalier, M. Saâdaoui, G. Fantozzi, M. Nawa, L.A. Diaz, R. Torrecillas, Fracture toughness, strength and slow crack growth in a ceria stabilized zirconia–alumina nanocomposites for medical applications, Biomaterials 29 (2008) 3636–3641.
[13] Y.B. Qiao, F.F. Jian, Q. Bai, Bioconjugation of zirconium uridine monophosphate: application to myoglobin direct electrochemistry, Biosens. Bioelectron. 23 (2008) 1244–1249.
[14] N.N. Zhu, A.P. Zhang, Q.J. Wang, P.G. He, Electrochemical detection of DNA hybridization using methylene blue and electro-deposited zirconia thin films on gold electrode, Anal. Chim. Acta 510 (2004) 163–168.
[15] Y.H. Song, L. Wang, C.B. Ren, G.Y. Zhu, Z. Li, A novel hydrogen peroxide sensor based on horseradish peroxidase immobilized in DNA films on a gold electrode, Sens. Actuators B: Chem. 114 (2006) 1001–1006.
[16] A.K.M. Kafi, F. Yin, H.K. Shin, Y.S. Kwon, Hydrogen peroxide biosensor based on DNA-Hb modified gold electrode, Thin Solid Films 499 (2006) 420–424.
[17] Y.M. Lvov, Z. Lu, J.B. Schenkman, X. Zu, J.F. Rusling, Direct electrochemistry of myoglobin and cytochrome P 450_{cam} in alternate layer-by-layer films with DNA and other polyions, J. Am. Chem. Soc. 120 (1998) 4073–4080.
[18] X. Liu, Y. Huang, G. Li, Enhanced electron transfer reactivity of horseradish peroxidase in phosphatidylcholine films and its catalysis to nitric oxide, J. Biotechnol. 108 (2004) 145–152.
[19] E. Antonini, M. Brunori, Hemoglobin and Myoglobin in Their Reactions with Ligands, North-Holland, Amsterdam, 1971.
[20] E. Katz, I. Willner, Probing biomolecular interactions at conductive and semiconductive surfaces by impedance spectroscopy: routes to impedimetric immunosensors, DNA-sensors, and enzyme biosensors, Electroanalysis 15 (2003) 913–947.
[21] X.S. Yang, X. Chen, J.H. Zhang, W.S. Yang, Fabrication of electroactive layer-by-layer films of myoglobin and zirconium phosphate nanosheets, Chem. Lett. 37 (2008) 240–241.
[22] A.J. Bard, L.R. Faulkner, Electrochemical Methods: Fundamentals and Applications, Wiley, New York, 2001.
[23] J. Kendrew, D. Phillips, V. Stone, Structure of myoglobin: a three-dimensional Fourier synthesis at 2 Å resolution, Nature 185 (1960) 422–427.
[24] C.P. Andrieux, C. Blocman, J.M. Dumas-Bouchiant, J.M. Saveant, Heterogeneous and homogeneous electron transfers to aromatic halides: an electrochemistry redox catalysis study in the halobenzene and halopyridine series, J. Am. Chem. Soc. 101 (1979) 3431–3441.
[25] G. Zhao, J.J. Feng, J.J. Xu, H.Y. Chen, Direct electrochemistry and electrocatalysis of heme proteins immobilized on self-assembled ZrO_2 film, Electrochem. Commun. 7 (2005) 724–729.

Biographies

Yuanbiao Qiao received his MS degree from Wuhan University in 2004. He achieved his doctor's degree in 2007 from New Materials and Function Coordination Chemistry Laboratory, Qingdao University of Science and Technology. He is now a postdoctoral candidate in Institute of Bioengineering, College of Materials Science and Engineering, Zhejiang University. His current researches are biocatalysis and biotransformation.

Guang Yang is now a doctoral candidate in Institute of Bioengineering, College of Materials Science and Engineering, Zhejiang University. Her current researches are biocatalysis and biotransformation.

Fangfang Jian received his postdoctoral degree from Nanjing University of Science and Technology in 2002. He is now a professor in New Materials and Function Coordination Chemistry Laboratory, Qingdao University of Science and Technology. His current interest is bioinorganic chemistry.

Yongqi Qin finished his doctoral study in 2008 from New Materials and Function Coordination Chemistry Laboratory, Qingdao University of Science and Technology. His current interest is bioinorganic chemistry.

Lirong Yang is a professor in Institute of Bioengineering, College of Materials Science and Engineering, Zhejiang University. His current researches are biocatalysis and biotransformation. He is now the Project Leader of the Chinese National Natural Science Foundation, a Key Project Leader of Chinese National Programs for Fundamental Research and Development, and a Leader for the Hi.-Tech. Research and Development Program of China, respectively.